**Title:** Floating photovoltaics could mitigate climate change impacts on water body temperature and stratification

**Author names and affiliations**

Giles Exley[a**], Alona Armstrong[a,b], Trevor Page[a], Ian D. Jones[c]

[a]Lancaster Environment Centre, Library Avenue, Lancaster University, Lancaster, LA1 4YQ, UK

[b]Energy Lancaster, Science & Technology Building, Lancaster University, Lancaster, LA1 4YF, UK

[c]Biological and Environmental Sciences, University of Stirling, Stirling, FK9 4LA, UK

[**]Corresponding author: g.exley@lancaster.ac.uk

**Abstract**

Floating solar photovoltaics, or floatovoltaics (FPV), are a relatively new form of renewable energy, currently experiencing rapid growth in deployment. FPV decarbonises the energy supply while reducing land-use pressures, offers higher electricity generating efficiencies compared to ground-based systems and reduces water body evaporation. However, the effects on lake temperature and stratification of FPV both sheltering the water's surface from the wind and limiting the solar radiation reaching the water column are unresolved, despite temperature and stratification being key drivers of the ecosystem response to FPV deployment. These unresolved impacts present a barrier to further deployment, with water body managers concerned of any deleterious effects. To overcome this knowledge gap, here the effects of FPV-induced changes in wind speed and solar radiation on lake thermal structure were modelled utilising the one-dimensional process-based MyLake model. To resolve the effect of FPV arrays of different sizes and designs, observed wind speed and solar radiation were scaled using a factorial approach from 0 % to 100 % in 1 % intervals. The simulations returned a highly non-linear response, dependent on system design and coverage. The responses could be either positive or negative, and were often highly variable, although, most commonly, water temperatures reduce, stratification shortens and mixed depths shallow. Modifications to the thermal dynamics of the water body may subsequently drastically alter biogeochemical processes, with fundamental implications for ecosystem service provision and water treatment costs. The extreme nature of response for particular wind speed and solar radiation combinations results in impacts that could be comparable to, or more significant than, climate change. As such, depending on how they are used, FPV have the potential to mitigate some of the impacts of climate change on water bodies and could be a useful tool for water body managers in dealing with changes to water quality, or, conversely, they could induce deleterious impacts on

standing water ecosystems. These simulations provide a starting point to inform the design of future systems that maximise ecosystem service and environmental co-benefits from this growing water body change of use.

**Keywords:** Floating solar, floatovoltaics, renewables, mixed depth, ecosystem impacts, lake management

**Graphical Abstract**

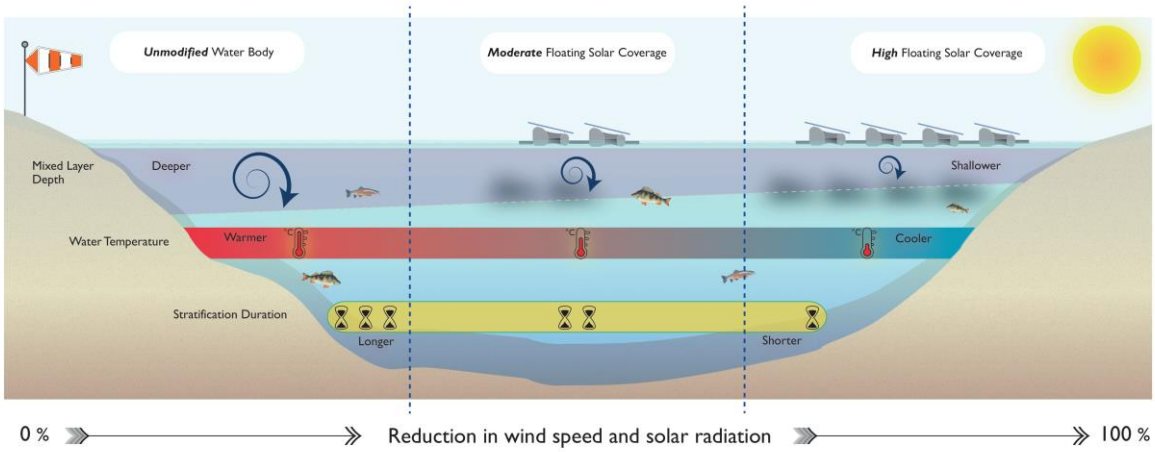


**Word Count:** 5453

# 1 Introduction

Increased energy demands and the urgent need to decarbonise are prompting the rapid deployment of renewable energy technologies. One such technology, solar photovoltaics (PV), has experienced exponential growth over the past 25 years (IEA, 2019) and accounted for 57 % of newly installed renewable energy capacity in 2019 (REN21, 2020). While solar PV has traditionally been ground- or rooftop-mounted, water-deployed, floating solar photovoltaics (FPV), known colloquially as floatovoltaics, have emerged in recent years. Global cumulative FPV capacity more than trebled among the top 70 FPV systems from 2018 to 2019 (Solar Asset Management, 2018; Solarplaza, 2019; World Bank Group et al., 2019), with a forecasted annual average growth rate of 22 % (Cox, 2019). Conservative estimates suggest that FPV has a global potential of 400 GW-peak (World Bank Group et al., 2018), demonstrating the likely widespread uptake of this renewable energy technology. Although this could be severely hampered by a lack of understanding about the impacts of the technology on the hosting environment (Gorjian et al., 2021; Lee et al., 2020; Stiubiener et al., 2020; Zhang et al., 2020; Ziar et al., 2020).

FPV systems are typically comprised of five main components: a pontoon of floaters, a mooring system, PV modules, cabling, and connectors (Sahu et al., 2016). The specific design of a system can be adapted to suit water body function and application through variations to floater material (Oliveira-Pinto and Stokkermans, 2020), PV module type (Tina et al., 2021; Ziar et al., 2020), orientation (Campana et al., 2019), and surface coverage (Cagle et al., 2020). However, each combination of components will have a unique impact on the atmospheric drivers of lake dynamics, potentially resulting in a large variation in lake function impacts between systems.

A growing body of evidence suggests that FPV has several advantages over conventionally deployed PV. Firstly, FPV averts the need for large areas of land-use change by occupying the surface of water bodies (Cagle et al., 2020; Holm, 2017). This is of particular benefit to land-scarce countries and regions with high land prices (Abid et al., 2019; Campana et al., 2019). Secondly, FPV has been shown to deliver enhanced performance over ground-based PV due to the cooling effect of the hosting water body (Choi et al., 2013; Oliveira-Pinto and Stokkermans, 2020; Sacramento et al., 2015; Yadav et al., 2016). The cooling yield has been found to vary across climates, with heat loss dependent on wind speed and the openness of the floating structure (Dörenkämper et al., 2021). Thirdly, and also dependent on system design, FPV has also been shown to reduce evaporative losses substantially (Choi, 2014; Sahu et al., 2016; Santafe et al., 2014; Taboada et al., 2017), potentially providing vital water savings for drought-stricken areas. Furthermore, studies have shown that hydroelectric dams operating in conjunction with FPV can optimise energy efficiency and

improve system reliability (Stiubiener et al., 2020; Zhou et al., 2020). Integrated hydroelectric-FPV systems may also lessen the environmental and social impacts of stand-alone hydroelectric operation (Sulaeman et al., 2021) providing synergistic benefits to the water-food-energy nexus (Zhou et al., 2020).

Nonetheless, the biological, chemical and physical impacts of FPV on water bodies remain virtually unknown (Ziar et al., 2020), despite the global importance of water bodies for supplying numerous ecosystem goods and services (Grizzetti et al., 2019; Maltby et al., 2011; Reynaud and Lanzanova, 2017). Given the forecasted growth in FPV deployment, it is critical that we increase our understanding of its impact on water bodies. A fundamental starting point to this understanding is recognising the impacts of FPV on the thermal structure of a water body, as this thermal structure will be directly affected by FPV and it has a pervasive influence on most other aspects of the ecosystem (e.g. Diehl et al., 2002; Huisman et al., 2004; Jäger et al., 2008; Macintyre, 1993).

A small number of previous studies have considered the effects of natural or artificial floating elements on lakes (e.g. Maestre-Valero et al., 2013; Ozkundakci et al., 2016). However, their focus has typically been on specific surface coverage ratios (e.g. Aminzadeh et al., 2018) or particular ecological effects such as phytoplankton and zooplankton assemblages (e.g. Cazzanelli et al., 2008; Pinto et al., 2007). Present understanding relating specifically to the ecological impacts of FPV on lake functioning is limited, with studies typically focussed on technological advancements and system implementation (e.g. Liu et al., 2017). Of the limited number of studies with an ecological focus, topics include; the viability of FPV on fish ponds (Chateau et al., 2019); the effect of novel FPV designs on water quality indicators at an FPV pilot site (Ziar et al., 2020) and the potential impact of sunlight reduction on biological processes, such as algal blooms (Haas et al., 2020) and microorganism proliferation in drinking water reservoirs (Mathijssen et al., 2020). Up to now, the impacts of FPV on water body thermal structure remains unexamined.

FPV will both reduce the amount of solar radiation reaching the water and shelter the water from the effects of wind mixing (Armstrong et al., 2020), modifying water body temperature and stratification. Wind speed and solar radiation typically have opposite effects on water body thermal structure. Decreases in wind will tend to increase stratification and surface warming, while reductions in solar radiation will enhance mixing and cooling of surface water (Kalff, 2002). At present, it remains unclear whether FPV-induced changes in wind speed or solar radiation will dominate, as well as the extent of any resulting changes to lake thermal structure. The critical role of temperature and stratification in determining lake biochemical and ecological processes (Elci, 2008; Kraemer et al., 2017) means that without this knowledge, deployment of FPV risks inadvertently

altering the provisioning of ecosystem goods and services. This could derail future investment in FPV. Modifications to the processes, function and service delivery of water bodies with an FPV installation must be carefully managed to ensure the pathway to decarbonisation continues with minimal concomitant environmental impacts.

Here we address this knowledge gap by applying simulations from a one-dimensional, process-based model and data from a test lake in North West England. We simulate water temperature, mixed depth and stratification timing to (1) determine the sensitivity of a lake's thermal structure to FPV deployed at varying scale. We then (2) consider the potential ecosystem consequences and implications for lake management in a changing climate.

# 2 Methods

## 2.1 Site description

The impacts of FPV on lake thermal structure were modelled for the south basin of Windermere, a typical monomictic, mesotrophic, deep and temperate lake in the Lake District, North West England. The south basin of Windermere is long and narrow in shape – with a maximum depth of 42 m, a mean depth of 16.8 m and a surface area of approximately 6.7 $km^2$. As one of the most comprehensively studied lake systems in the world (Rooney and Jones, 2010), the wealth of understanding and availability of high-resolution meteorological and in-lake water temperature data make Windermere an excellent test system for this study (Maberly and Elliott, 2012).

## 2.2 Modelling methodology

### 2.2.1 MyLake

To resolve the effects of FPV on lake physical properties, we simulated lake variables by adapting an existing MATLAB model. *MyLake* v1.2 (Saloranta and Andersen, 2007) is a one-dimensional process-based model, used to simulate the daily vertical distributions of water body temperature, evaporation and instances of ice cover accurately. *MyLake* partitions horizontal layer volumes by exploiting interpolated lake bathymetric data, making it similar to other one-dimensional lake models. The lake water simulation part of the model is based on Ford and Stefan (1980), Riley and Stefan (1988) and Hondzo and Stefan (1993), while the ice simulation component is based on Leppäranta (1993) and Saloranta (2000). In brief, the model initially computes the temperature distribution of the lake for the 24-hour time-step, taking into account diffusive mixing processes and local heat fluxes. A sequential process then accounts for convective mixing, wind-induced mixing, the water-ice heat flux and the effect of river inflow (Saloranta and Andersen, 2007). The model has been successfully applied to various projects as a standalone simulation tool assessing lake

thermodynamics and ice regime (e.g. Livingstone and Adrian, 2009; Woolway, R. Iestyn et al., 2017). Predominantly, model parameters were kept as per the user manual (Saloranta and Andersen, 2004), with minor adjustments made during calibration (see Section 2.4).

### 2.2.2 Input data

Meteorological data, logged at 4-minute intervals using a Campbell Scientific CR10X data logger, were obtained from an Automatic Water Quality Monitoring Station (AWQMS) located at the deepest point of Windermere south basin for 2009. Specifically, air temperature (Skye Instruments SKH2012) was measured with a relative accuracy of ±0.35 °C; relative humidity (HOBO U23-001) with an accuracy of ±3 %; incoming short-wave radiation (Kipp & Zonen CMP6) with a relative accuracy of 5 %, and wind speed (Vector Instruments A100L2) was measured with an accuracy of 1 % for wind speeds >10.3 m $s^{-1}$ and an accuracy of up to 0.1 m $s^{-1}$ for wind speeds <10.3 m $s^{-1}$. Water temperature profiles were obtained from 12 stainless-steel sheathed platinum resistance thermometers (Labfacility PT100), accurate to within 0.1 °C at the following depths; 1, 2, 4, 7, 10, 13, 16, 19, 22, 25, 30 and 35 m. Data were averaged to daily time steps. Estimates for cloud cover (0-1) were obtained from the R package *insol* (Corripio, 2019), using incoming short-wave radiation data from the AWQMS. As *MyLake* requires air temperature and relative humidity at 2 m, and wind speed at 10 m, corrections for measurement height were applied using a modified version of *Lake Heat Flux Analyser* (Woolway et al., 2015b). An iteration scheme with a smoothing function capable of assessing bulk fluxes at individual time steps allowed the appropriate scheme to be applied for accurate bulk flux simulation.

Daily discharge data from Windermere (River Leven) were used as a proxy for inflow (National River Flow Archive, 2018), following the assumption that inflow was approximately matched by outflow, with negligible change in lake level. Lake morphometry (Ramsbottom, 1976) was interpolated to one-metre intervals. The light attenuation coefficient ($K_d$, $m^{-1}$) for Windermere south basin was obtained from Woolway et al. (2015a).

### 2.2.3 Thermal structure simulations

The effect on wind speed and solar radiation (forcing variables) for a given percentage coverage of FPV is unknown and likely to vary substantially depending on the design of the floatovoltaic deployment. While reductions to both forcing variables are likely, the relative proportions of these reductions remain to be determined. Here, the forcing variables were altered using a factorial design, simulating reductions at 1 % intervals from 0 % to 100 %. A factorial design allowed the identification of non-linear changes and thresholds in the output variables; this was of particular importance given the range of FPV designs and surface coverages that exist between different

systems. Considering reductions to the forcing variables as a whole lake average, not just in the footprint of the array, maximises transferability between systems with different FPV designs.

## 2.3 Data Analysis

Mixed layer depth and Schmidt stability were subsequently estimated from modelled water temperatures using *Lake Analyzer* (Read et al., 2011), a freely available physical limnological tool (e.g. Kraemer et al., 2015; Read et al., 2012). Mixed layer depth was estimated using the metalimnion extent function, an algorithm that defines the approximate depth of the base of the mixed layer using a density gradient threshold of 0.1 kg $m^{-3}$ $m^{-1}$. Mean mixed layer depth for the stratified period of each scenario, along with annual mean mixed layer depth were calculated.

The onset of thermal stratification was defined from the depth-resolved temperature simulations as the time when the temperature differential between the surface (0 m) and the bottom (42 m) of the lake exceeded 1 °C (Fee et al., 1996). Alterations to stratification duration were assessed by calculating the longest stratified period, defined here as the greatest number of consecutive days of stratification across the simulated period. This was then compared to the stratified period of the water body without FPV (unmodified system), permitting the calculation of a gain or loss in stratified days. Stratification onset and overturn days were derived from these data, with onset being the first day and overturn being the final day of the longest stratified period.

Three simulation scenarios were considered in further detail. The first being an equal (1:1) reduction to each forcing variable. Given the relative proportions of reductions to forcing variables remain unknown and are likely to vary substantially depending on FPV design (see Section 2.2.3), two scenarios with scaled forcing variables were simulated. A ‘wind dominant’ scenario where the wind speed reduction scales as 80 % of the solar radiation reduction and a ‘solar dominant’ scenario where the reduction to solar radiation scales as 80 % of the wind speed reduction.

## 2.4 Model Calibration

The model was calibrated for a one-year period against observed water body temperatures. Standard calibration procedures were undertaken following Moriasi et al. (2007). Briefly, calibration of the scaling of forcing variables was guided by Monte Carlo sampling of uniform parameter distributions. The Nash-Sutcliffe model efficiency coefficient (NSE) (Nash and Sutcliffe, 1970) and the Root Mean Square Error (RMSE) for metalimnion top, Schmidt stability and volume average temperature (see supplementary information) were used to identify the best simulation. Slight modifications to scale the original driving data were required to achieve the optimum parameter values for the calibration year; these were +2 % for wind speed and +13 % for solar radiation. These modifications are within the instrumentation error range and help reflect the variation likely

experienced in forcing variables across the whole of the water body. Thus, driving the model using 2009 measured meteorological data with a wind speed multiplier of 1.02 and a solar radiation multiplier of 1.13 provided the optimum fit against the observed in-lake temperature data and this then constituted the baseline model simulation.

# 3 Results

After calibration, simulated water temperatures, volume averaged temperatures, mixed layer depth and Schmidt stability compared favourably to the observed data (Figure S1). Model efficiency computed with NSE ranged from 0.93 to 0.97, an encouraging indication of the ability of the model to reproduce the system response (see supplementary information for full calibration details, Table S1).

## 3.1 Response of water body temperature to FPV

Modelled reductions to the forcing variables generally reduced annual mean surface water temperatures (Figure 1a). Surface water temperature reductions were non-linear, with small reductions to the forcing variables having a negligible effect and larger reductions having an increasingly greater effect (Table S2). Increases in surface water temperatures occurred only in scenarios when wind speed was reduced considerably more than solar radiation. Similarly, annual mean bottom temperatures generally decreased, albeit less than surface temperatures (Figure 1b). As could be expected, given the reductions in surface and bottom water temperatures, mean annual volume average temperature was reduced for all scenarios (Figure S2).

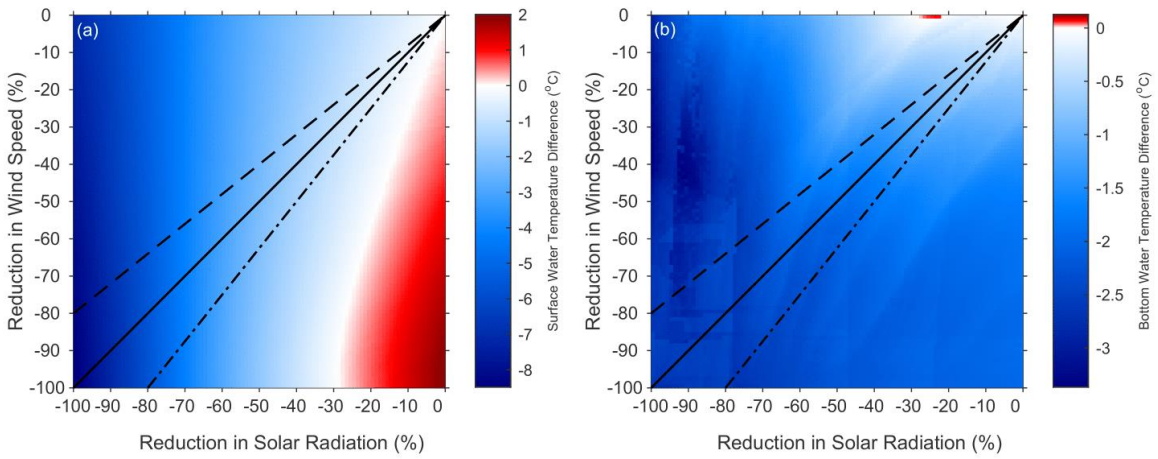


*Figure 1 - Differences in mean surface and bottom water temperatures. Results are shown for mean annual (a) surface water temperature and (b) bottom water temperature. Water temperatures for the unmodified system were (a) 11.2 °C and (b) 7.0 °C. The solid black line represents an equal wind speed and solar radiation reduction approximating floating solar coverage (1:1). A wind dominant scenario (solar radiation reduced more than wind speed) is shown with a dashed line. The dot-dash line represents a solar dominant scenario (wind speed reduced more than solar radiation).*

In 2009 there was no ice-cover on the lake and, indeed, ice cover on Windermere is very rare. Nevertheless, simulations with more than a 90 % reduction to the forcing variables resulted in sufficiently cold surface water temperatures for ice to form (Figure S3). Ice cover duration increased as the forcing variables were further reduced above 90 %. For example, a 90 % 1:1 reduction resulted in 22 days of ice cover, while a 98 % reduction resulted in 43 days of ice cover.

Each reduction to the forcing variables decreased total annual evaporation in comparison to the baseline (Figure 2). At a 74 % 1:1 forcing variable reduction, a threshold was crossed where dew formed on the lake surface, providing an annual net gain in water. Wind dominant scenarios (solar reduced by more than wind) saw greater reductions in evaporation than in solar dominant scenarios (Table S2).

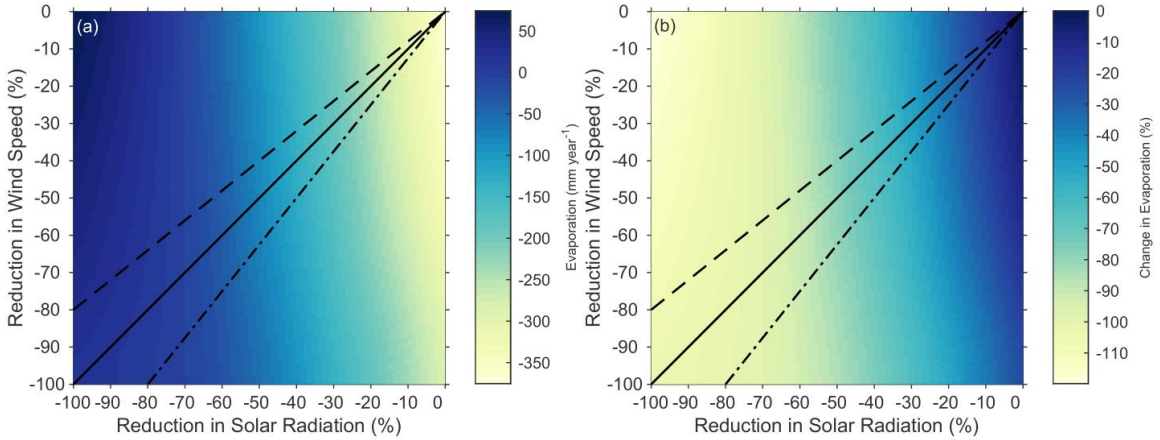


*Figure 2 - Annual evaporation and change in evaporation. Results are shown for (a) total annual evaporation. A negative value indicates a net loss of water from the lake, while a positive value indicates a net gain in water. (b) The percentage change in evaporation in comparison to the baseline (375.2 mm year$^{-1}$). The solid black line represents an equal wind speed and solar radiation reduction approximating floating solar coverage (1:1). A wind dominant scenario (solar radiation reduced more than wind speed) is shown with a dashed line. The dot-dash line represents a solar dominant scenario (wind speed reduced more than solar radiation).*

## 3.2 Response of stratification duration and strength to FPV

### 3.2.1 Stratification duration

When reductions to the forcing variables were 1:1 and did not exceed 45 %, stratification duration was similar (± three days) to that of Windermere without FPV (Figure 3). Reductions in excess of this threshold decreased stratification duration by ~39 days for every additional 10 % reduction to the forcing variables (Table S3a). However, when the reductions to the forcing variables were not 1:1, stratification duration was modified even with small reductions. A solar dominant scenario, for example, increased stratification duration for all scenarios up to a 52 % solar reduction, ranging from 3 to 13 days increase. The opposite was true when wind dominated, with stratification duration

decreasing for all scenarios by a minimum of 29 days, up to a maximum of 214 days. Solar radiation reductions tended to dominate over wind speed reductions in determining stratification duration.

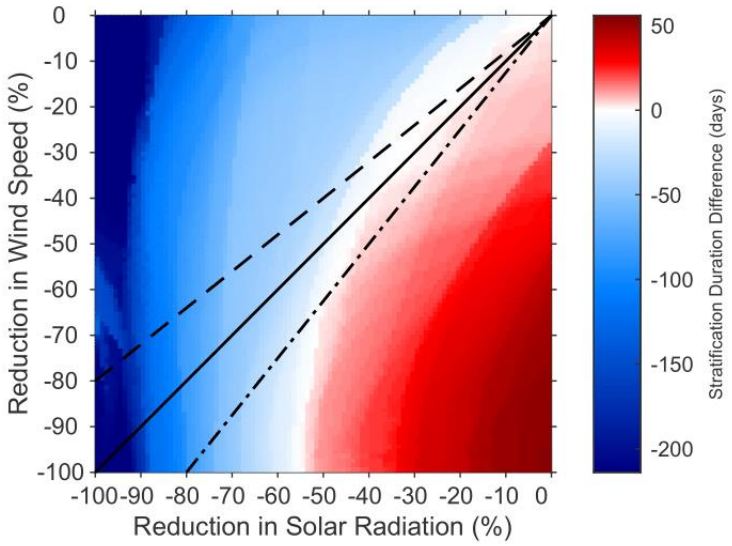


*Figure 3 - Stratification duration for each scenario. The unmodified system was stratified for 214 days. The solid black line represents an equal wind speed and solar radiation reduction approximating floating solar coverage (1:1). A wind dominant scenario (solar radiation reduced more than wind speed) is shown with a dashed line. The dot-dash line represents a solar dominant scenario (wind speed reduced more than solar radiation).*

### 3.2.2 Stratification Onset & Overturn

FPV deployment shifted the stratified period to later in the year, with delayed onset and overturn (Table S3a, b). Wind dominant scenarios typically delayed stratification, where wind speeds remained proportionally higher than solar radiation (dashed-line Figure 4a). However, in scenarios where the wind speed was reduced by at least 30 %, but solar radiation remained little changed, onset occurred earlier in the year. Overturn was delayed by up to 10 days as a consequence of reduced wind speed when 1:1 forcing variable reductions were less than 72 %. Above 72 %, the dominant forcing variable switched, with reduced solar radiation advancing overturn timing (Figure 4b).

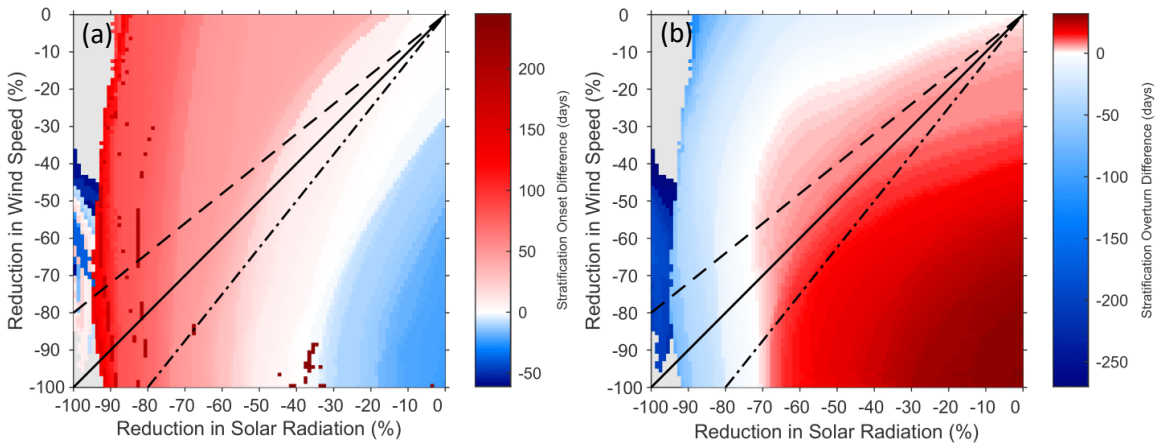


*Figure 4 - Stratification onset and overturn. Change in day of year shown for (a) onset and (b) overturn of thermal stratification with modified wind speed and solar radiation. A negative value indicates an earlier day of the year (advancement), while a positive value indicates a later day of the year (postponement). Stratification onset and overturn occurred at day 102 and 315 respectively. The solid black line represents an equal wind speed and solar radiation reduction approximating floating solar coverage (1:1). A wind dominant scenario (solar radiation reduced more than wind speed) is shown with a dashed line. The dot-dash line represents a solar dominant scenario (wind speed reduced more than solar radiation).*

### 3.2.3 Stability

Forcing variable reductions of up to 13 % modified Schmidt stability by a relatively modest ±10 J $m^{-2}$, within 3 % of the unmodified system. Scenarios where FPV reduced forcing variables by more than 13 % reduced Schmidt stability substantially (Figure S4). The stability of the water body only increased in instances when wind speed was reduced considerably, with solar radiation reduced by no more than 20 %. A 10 % solar radiation reduction and a 50 % wind speed reduction, for example, increased mean annual Schmidt stability by 59 J $m^{-2}$. When each forcing variable was reduced by 50 %, Schmidt stability was reduced by 126 J $m^{-2}$. Solar radiation changes were generally the dominant factor determining Schmidt stability, seen by the vertical bands in Figure S4; changing the wind speed had less influence, especially at higher reductions of solar radiation.

## 3.3 Mixed Depth

Annual mean mixed depth shallowed with 1:1 forcing variable reductions of up to 60 % (1:1) (Table S4a), indicated by the negative mixed depth difference. Reductions greater than 60 % (1:1) deepened the annual mean mixed depth, with the water body remaining mixed all year when reductions exceeded 94 % (1:1) (Figure 5a, b). Mixed depth was shallowed by 0.58 m for every 10 % reduction to the forcing variables up to 40 % (1:1).

These changes in annual mixed depth were, in part, caused by the changes in stratification duration. Excluding this effect by focussing only on the stratified period, each scenario demonstrated a

shallowing of mean summertime mixed depth for all 1:1 reductions (Figure 5c, d). Reductions in excess of 81 % were highly non-linear (1:1), while smaller reductions were relatively proportional to the forcing variable reduction. The effect of FPV on mixed depth was considerable, with 85 % of all scenarios shallowing for the stratified period (Table S4b). Net summertime deepening occurred for the remaining scenarios, typically when very large changes to solar radiation were coupled with only small changes to wind speed. Mixed depth was at least halved for 29 % of all scenarios.

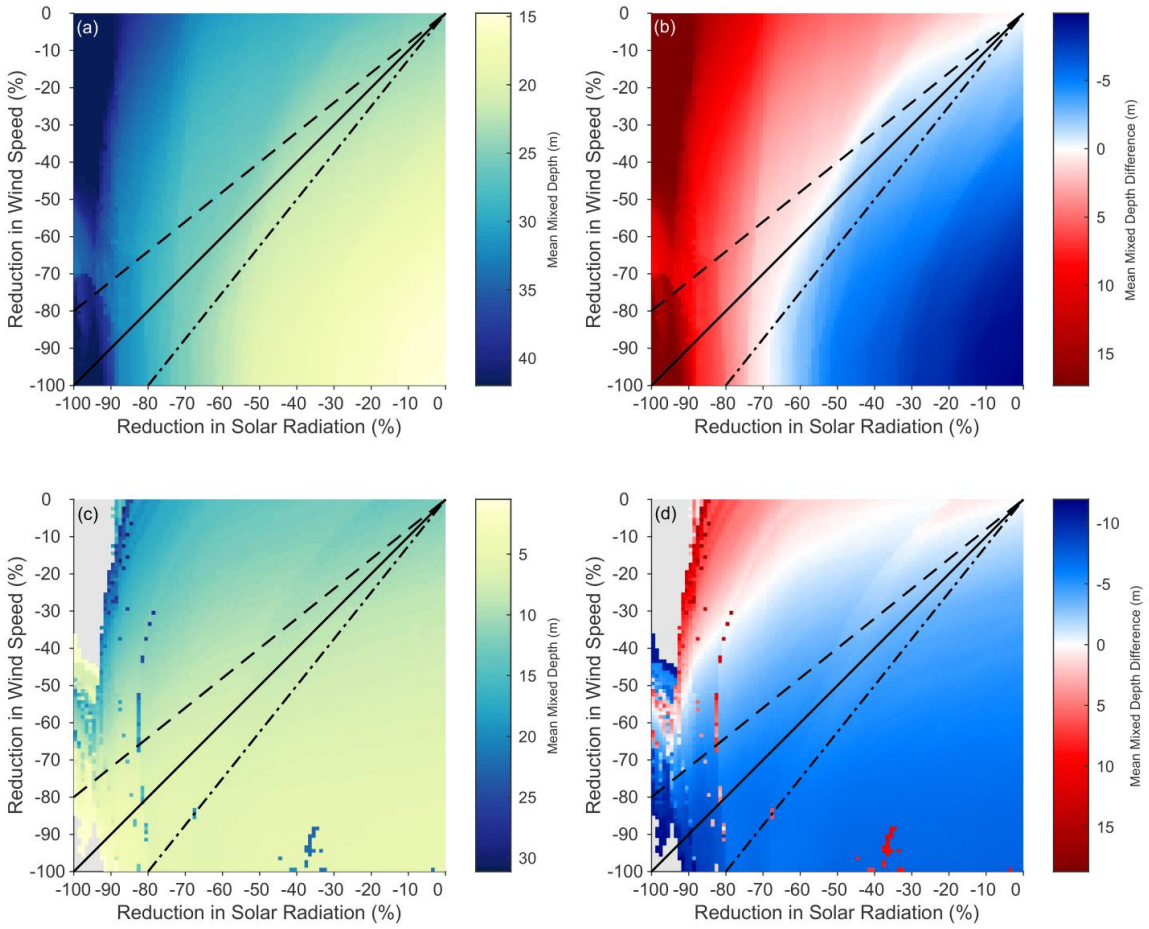


*Figure 5 - Annual and stratified period mixed depths for each scenario. Results shown for (a) annual mean mixed depth, (b) difference from the baseline for annual mean mixed depth, (c) mean mixed depth for the stratified period and (d) the difference in mean mixed depth for the stratified period of each scenario with modified wind speed and solar radiation. A negative value on (b) or (d) indicates mixed depth has shallowed, i.e. has moved closer to the surface of the water body. A positive value on (b) or (d) indicates a deepening of mixed depth, i.e. mixed depth has shifted towards the bottom of the water body. Annual and stratified period mean mixed layer depth were 24.7 m and 12.4 m, respectively. The solid black line represents an equal wind speed and solar radiation reduction approximating floating solar coverage (1:1). A wind dominant scenario (solar radiation reduced more than wind speed) is shown with a dashed line. The dot-dash line represents a solar dominant scenario (wind speed reduced more than solar radiation).*

There were strong seasonal dynamics in mixed depth, with progressive deepening throughout the summer months for scenarios where forcing variables were reduced by up to 75 % (1:1) (Table S5;

Figure 6). Daily mixed depths, for scenarios with forcing variable reductions of 5, 10, 25, 50 and 75 % (1:1) were initially closely aligned to the mixed layer depth of the unmodified system (Figure 6). At day 175 (24/06/09) the mixed depth of each scenario diverged from the unmodified system before converging again at day 325 (21/11/09). During the diverged period, scenarios with forcing variable reductions of 10 % or greater differed substantially from the unmodified system, with mean mixed depths differing by more than 2 m. Although the trend remained consistent, the magnitude did vary. The difference in mixed depth peaked at 15.4 m for the 75 % scenario on day 305 (01/11/09). A 100 % (1:1) reduction to the forcing variables kept the water body fully mixed throughout the entire year.

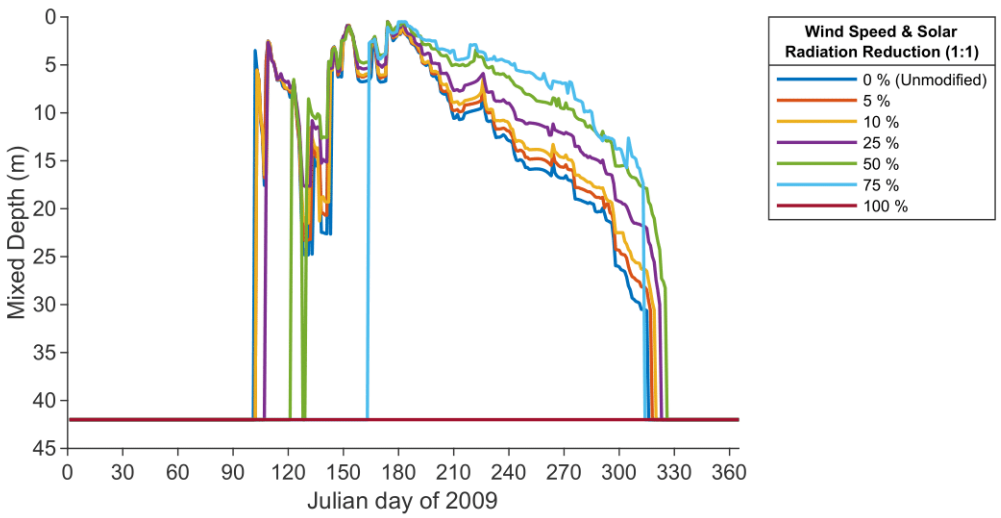


*Figure 6 - Daily mixed depth. The scenarios shown have equal wind speed and solar radiation reductions approximating floating solar coverage (1:1).*

# 4 Discussion

Lake thermal structure is dependent on a range of factors, including weather conditions, lake morphology and geographical location (Kalff, 2002). Although FPV deployments will alter net wind speed and solar radiation at the lake surface, the simulations here did not assume a specific extent of coverage or system design. Instead, we considered the effects of varying the scale of the forcing variables. For this discussion, we use only the assumption that surface coverage is negatively correlated with the forcing variables, i.e. that higher surface coverages cause a greater reduction in wind speed and solar radiation.

Thermal responses to differing reductions in wind speed and solar radiation varied enormously, from the negligible to the very large. Proportionate increases in alteration of driving forces resulted in highly non-linear responses. Both positive and negative responses were possible, depending on the

changes to the driving variables, reflecting the opposite effects that wind speed and solar radiation typically have on lake thermal structure. The responses most commonly seen, though, were for temperatures to reduce, stratification to shorten, but mixed depths to become shallower. In the small number of instances when water temperature increased or stratification duration lengthened, an FPV system would need to cause substantial wind speed reductions and minimal solar radiation reductions. Conversely, the rare instance of mixed depth deepening (when considered during the stratified period only) occurred when substantial solar radiation reductions were coupled with minimal wind speed reductions.

## 4.1 The sensitivity of lake thermal structure to FPV

### 4.1.1 Cooling effect on water temperature

Water temperature changes were minor for small coverages of FPV, while more extensive FPV coverages drove major decreases (Figure 1). As many metabolic processes are highly temperature-dependent, the deployment of FPV at large coverages has the potential to change the functioning of lentic ecosystems by modifying animal behaviour, food web dynamics, life histories, species interactions and carbon cycling (Kraemer et al., 2017; Tranvik et al., 2009). Reduced water temperatures may also present operational challenges, particularly to networks comprised of cast iron distribution mains. During the colder winter months, increased tensile stresses from reduced water temperatures may lead to pipe fractures and an increased incidence of pipe bursts (Jesson et al., 2010).

Cooler water temperatures and greatly reduced wind speeds permitted the formation of ice at high surface coverages (Figure S3), shifting the lake from a monomictic to a dimictic stratification regime. This considerable temporal shift in ice cover regime may have implications for cyanobacterial community composition (Ozkundakci et al., 2016) and fish behaviour (Jurvelius and Marjomki, 2008) while enhancing cultural ecosystem service provisioning (Knoll et al., 2019). In water bodies where FPV deployment could induce ice-cover, consideration would need to be given in the FPV design to mitigate the possibilities of compression forces and the restriction of array movement due to ice cover.

### 4.1.2 Changes to stratification length

Typically, the interception of incoming solar radiation by FPV extended the period of water column heating required in the spring before a density gradient established, postponing thermal stratification onset (Figure 4). Delayed epilimnion formation has been shown to shift the timing of spring phytoplankton blooms to later in the year (Meis et al., 2009), a phenological

desynchronization which could lead to trophic mismatch, affecting the wider food web hierarchy (Thackeray et al., 2013; Visser and Both, 2005).

At low to moderate FPV coverages, stratification duration increased a little, and more so when wind reductions were substantially greater than solar radiation reductions (Figure 3), increasing the likelihood of hypolimnetic anoxia and the increased regeneration of soluble phosphorus and metals from the lake sediment (Beutel et al., 2008; Forsberg, 1989). The regeneration of heavy metals from lakebed sediment degrades water quality, necessitating enhanced water treatment, although the postponement of overturn may mean extra nutrient releases occur at periods of lower light availability when conditions are less suitable for phytoplankton growth (Butcher et al., 2015). At higher FPV coverages and scenarios with enhanced solar reduction, stratification duration shortened, which would tend to have the opposite effect of reducing anoxia and internal loading of nutrients and metals. The possibility of either outcome, increase or decrease, for such critical components of water quality emphasises the need for astute system design.

### 4.1.3 Alteration of mixed layer depth

While it was more common in the model results that water temperature was lowered, stability reduced and stratification shortened, mixed layers typically were shallowed, not deepened (Figure 5). Thus, reductions in solar radiation seemed to be more influential than wind speed reductions on water temperature and stratification, but the reduction in wind speed more influential on the depth of the epilimnion. As a fundamental driver of the chemistry and biology of lake ecosystems, the modification of mixed layer depth by FPV is of considerable importance for water quality (Kraemer et al., 2015; North et al., 2014; Yankova et al., 2017). FPV deployments will reduce photosynthetically active radiation (PAR) directly under array structures as well as mixed depth, so the ratio of epilimnetic depth to euphotic depth will alter, impacting phytoplankton growth (Huisman et al., 1999). Individual phytoplankton species with adaptations well suited to the modified epilimnetic depth to euphotic depth ratio beneath an FPV array will thrive, so changes in biomass and species composition should be expected. Non-continuous FPV deployments that allow a mosaic of light availability will complicate alterations to the phytoplankton community further. In particular, and of concern for water body managers, toxic cyanobacteria are well adapted to such conditions, utilising gas vesicles to regulate their buoyancy (Walsby et al., 1997). Simulations by Haas et al. (2020) found FPV systems that reduced light attenuation by 40 %, or more, greatly reduced algal biomass, although they did not consider the effects of reduced wind speed, which may improve conditions for phytoplankton growth. The use of semi-transparent PV modules which provide specific transmittance windows to control light intensities have been proposed as a means to regulate phytoplankton growth (Zhang et al., 2020).

## 4.2 FPV and lake management in the context of a changing climate

The deployment of FPV is a direct response to the need to decarbonise the global energy supply in order to avert catastrophic climate change. Simulations here demonstrate that the effects on lake thermal structure of certain combinations of forcing variable reduction can be as, or more influential, than effects induced by climate change, and could either mitigate or exacerbate the impact. Numerous studies have identified increasing lake temperatures due to climate change, which are predicted to disturb both ecological and biogeochemical processes (e.g. O'Neil et al., 2012; Paerl and Paul, 2012; Thackeray et al., 2008). Woolway et al. (2019) found the average annual minimum surface-warming rate of eight lakes to be 0.35 °C decade$^{-1}$, while O'Reilly et al. (2015) found 235 globally distributed lakes' summer surface water temperatures were warming at a mean trend of 0.34 °C decade$^{-1}$. Thus, FPV may provide a useful tool for water body managers in mitigating against lake warming. For example, a decade of lake surface temperature warming could be mitigated with the deployment of an FPV array at a surface coverage that reduces lake-average wind speed and solar radiation by approximately 10 % (Figure 1).

A further example of climate change mitigation, and of particular relevance to water-scarce locations, is the reduction in evaporation achieved by increasing FPV coverage (Figure 2). Cooler surface water temperatures weaken the water-to-air vapour pressure difference (Oke, 2002) while the FPV array intercepts incoming radiative energy, reducing the latent heat flux (Aminzadeh et al., 2018). Although research has previously identified that FPV will reduce evaporative losses (e.g. Ferrer-Gisbert et al., 2013; Redón-Santafé et al., 2014; Taboada et al., 2017), here it is also shown that the cooler surface water under FPV relative to the warmer, moist air above the water body permits dew deposition (Oke, 2002). At coverages greater than 74 % (1:1 forcing variable reduction) a tipping point is crossed, resulting in a net gain of water to the lake.

However, while FPV could be an effective tool to mitigate against lake warming, FPV facilitated prolonged stratification duration and delayed overturn for some scenarios simulated in this study, with the potential consequences similar to those of climate warming (e.g. Adrian et al., 1995; Woolway and Merchant, 2019). Foley et al. (2012) examined long-term changes in stratification dynamics for a lake close to Windermere between 1968 and 2008; they found climate warming led to onset occurring 28 days earlier, overturn 18 days later, and the duration of stratification increased by 38 days. While FPV may be able to lessen the earlier onset of stratification brought about by climate change, the simulations show FPV deployment at lower coverages may also exacerbate the effects of climate change, potentially lengthening stratification duration and postponing overturn further.

## 4.3 FPV deployment best practice

These simulations show impacts on water body process and function in response to the deployment of FPV, with results which are relevant for other monomictic and mesotrophic deep lakes in the temperate zone, although variations in local climate may constrain or exacerbate many of the effects identified in this study. Any wider extrapolation of these impacts needs to take into consideration geographical and morphological factors that affect lake-atmosphere interactions. For example, ice cover, which occurred with high FPV coverage rates, would not occur in tropical regions due to higher air temperatures. Lakes in tropical regions also undergo different mixing regimes and tend to have less vertical temperature difference than temperate lakes (Lewis, 1987), so may respond differently to a temperate system. As latitude also influences turbulent surface heat fluxes (Woolway et al., 2018) and atmospheric stability above lakes (Woolway, et al., 2017), geographical location is likely to be a key contributor to the overall effect of FPV on lake thermal structure. The response of lakes with differing morphometric characteristics must also be considered; lake surface area, volume and mean depth are pertinent drivers of lake thermal structure (Kraemer et al., 2015; Lerman et al., 1995; Talling, 2001; Wetzel, 2001). In smaller lakes, convection is the dominant driver of mixed-layer turbulence, while wind shear is the primary driver for larger lakes (Read et al., 2012). Lakes of a smaller surface area have broader diel temperature ranges than larger lake-systems making them more prone to disturbance (Woolway et al., 2016). The temporal variation in these drivers will further modify the response between individual systems.

The number of water bodies hosting FPV arrays will increase with the sustained global drive to decarbonise energy supplies; therefore, we anticipate an urgent need for further understanding on the effects of FPV. Critically the model simulations demonstrate a high sensitivity to extent and design of deployments with highly non-linear thermal responses and both increases or decreases in temperature and stratification being possible. The model simulations suggest only a few percent cover (< 10 %) of FPV typically only induces minor changes, but more significant covers (> ~50 %) result in large temperature changes and very extensive modifications to stratification timing. The effects of FPV at larger coverages are of a similar magnitude to that of climate change. This considerable variation in possible response provides those deploying FPVs an opportunity to utilise deployments for actively enhancing water quality benefits as well as decarbonising electricity production.

# 5 Conclusion

By simulating the response of a lake to FPV deployed at varying extent, this study has demonstrated patterns of increased impact with increased perturbation, ranging from negligible to very large.

Based on these findings, future FPV designs should consider the following to maximise ecosystem co-benefits and limit potential harm:

- Reductions in wind speed and solar radiation as an average across the lake cause a non-linear, complex response with the direction of these effects dependent on FPV array design, including coverage density
- Low FPV surface coverages had a negligible effect on the thermal structure of the test system, while high coverages were a major disruptor of the archetypal thermal structure
- FPV deployments may have impacts that are as, or more, influential than catastrophic climate change, therefore providing an opportunity to manage the effects of climate change on lake systems actively
- Appropriate design and deployment of FPV will be required to mitigate the likelihood of hypolimnetic anoxia and to optimise changes in the composition of phytoplankton communities as FPV modifies lake thermal structure and light climate

FPV is a substantial perturbation to water body process and function. Deployment with minor impact is possible, but the infancy of knowledge on FPV necessitates planning and impact assessment on a system-by-system basis.

## Declaration of competing interest

The authors declare that they have no known competing financial interests or personal relationships that could have appeared to influence the work reported in this paper.

## Acknowledgements

Funding: This work was supported by the Natural Environment Research Council (grant number NE/R010226/1) and United Utilities, with GE's Industrial CASE studentship through the Envision Doctoral Training Partnership. AA was supported by a NERC Industrial Innovation Fellowship (grant number: NE/R013489/1).

# 6 References


Abid, M., Abid, Z., Sagin, J., Murtaza, R., Sarbassov, D., Shabbir, M., 2019. Prospects of floating photovoltaic technology and its implementation in Central and South Asian Countries. International Journal of Environmental Science and Technology 16(3), 1755-1762.

Adrian, R., Deneke, R., Mischke, U., Stellmacher, R., Lederer, P., 1995. A long-term study of the Heiligensee (1975-1992). Evidence for effects of climatic change on the dynamics of eutrophied lake ecosystems. Archiv für Hydrobiologie 133(3), 315-337.

Aminzadeh, M., Lehmann, P., Or, D., 2018. Evaporation suppression and energy balance of water reservoirs covered with self-assembling floating elements. Hydrol Earth Syst Sc 22(7), 4015-4032.

Armstrong, A., Page, T., Thackeray, S.J., Hernandez, R.R., Jones, I.D., 2020. Integrating environmental understanding into freshwater floatovoltaic deployment using an effects hierarchy and decision trees. Environmental Research Letters 15(11).

Beutel, M.W., Leonard, T.M., Dent, S.R., Moore, B.C., 2008. Effects of aerobic and anaerobic conditions on P, N, Fe, Mn, and Hg accumulation in waters overlaying profundal sediments of an oligo-mesotrophic lake. Water Res 42(8-9), 1953-1962.

Butcher, J.B., Nover, D., Johnson, T.E., Clark, C.M., 2015. Sensitivity of lake thermal and mixing dynamics to climate change. Climatic Change 129(1-2), 295-305.

Cagle, A.E., Armstrong, A., Exley, G., Grodsky, S.M., Macknick, J., Sherwin, J., Hernandez, R.R., 2020. The Land Sparing, Water Surface Use Efficiency, and Water Surface Transformation of Floating Photovoltaic Solar Energy Installations. Sustainability 12(19).

Campana, P.E., Wasthage, L., Nookuea, W., Tan, Y.T., Yan, J.Y., 2019. Optimization and assessment of floating and floating-tracking PV systems integrated in on- and off-grid hybrid energy systems. Solar Energy 177, 782-795.

Cazzanelli, M., Warming, T.P., Christoffersen, K.S., 2008. Emergent and floating-leaved macrophytes as refuge for zooplankton in a eutrophic temperate lake without submerged vegetation. Hydrobiologia 605, 113-122.

Chateau, P.A., Wunderlich, R.F., Wang, T.W., Lai, H.T., Chen, C.C., Chang, F.J., 2019. Mathematical modeling suggests high potential for the deployment of floating photovoltaic on fish ponds. Sci Total Environ 687, 654-666.

Choi, Y.-K., 2014. A study on power generation analysis of floating PV system considering environmental impact. Republic of Korea.

Choi, Y.-K., Lee, N.-H., Kim, K.-J., 2013. Empirical Research on the efficiency of Floating PV systems compared with Overland PV Systems, Proceedings, The 3rd International Conference on Circuits, Control, Communication, Electricity, Electronics, Energy, System, Signal and Simulation. pp. 284-289.

Corripio, J.G., 2019. insol: Solar Radiation, 1.2 ed. CRAN.

Cox, M., 2019. Floating solar landscape 2019, Wood Mackenzie Power and Renewables.

Diehl, S., Berger, S., Ptacnik, R., Wild, A., 2002. Phytoplankton, light, and nutrients in a gradient of mixing depths: Field experiments. Ecology 83(2), 399-411.

Dörenkämper, M., Wahed, A., Kumar, A., de Jong, M., Kroon, J., Reindl, T., 2021. The cooling effect of floating PV in two different climate zones: A comparison of field test data from the Netherlands and Singapore. Solar Energy 214, 239-247.

Elci, S., 2008. Effects of thermal stratification and mixing on reservoir water quality. Limnology 9(2), 135-142.

Fee, E.J., Hecky, R.E., Kasian, S.E.M., Cruikshank, D.R., 1996. Effects of lake size, water clarity, and climatic variability on mixing depths in Canadian Shield lakes. Limnol Oceanogr 41(5), 912-920.

Ferrer-Gisbert, C., Ferran-Gozalvez, J.J., Redon-Santafe, M., Ferrer-Gisbert, P., Sanchez-Romero, F.J., Torregrosa-Soler, J.B., 2013. A new photovoltaic floating cover system for water reservoirs. Renew. Energy 60, 63-70.

Foley, B., Jones, I.D., Maberly, S.C., Rippey, B., 2012. Long-term changes in oxygen depletion in a small temperate lake: effects of climate change and eutrophication. Freshwater Biology 57(2), 278-289.

Ford, D.E., Stefan, H.G., 1980. Thermal Predictions Using Integral Energy-Model. J Hydr Eng Div-Asce 106(1), 39-55.

Forsberg, C., 1989. Importance of Sediments in Understanding Nutrient Cyclings in Lakes. Hydrobiologia 176(1), 263-277.

Gorjian, S., Sharon, H., Ebadi, H., Kant, K., Scavo, F.B., Tina, G.M., 2021. Recent technical advancements, economics and environmental impacts of floating photovoltaic solar energy conversion systems. Journal of Cleaner Production 278, 124285.

Grizzetti, B., Liquete, C., Pistocchi, A., Vigiak, O., Zulian, G., Bouraoui, F., De Roo, A., Cardoso, A.C., 2019. Relationship between ecological condition and ecosystem services in European rivers, lakes and coastal waters. Sci Total Environ 671, 452-465.

580 Haas, J., Khalighi, J., de la Fuente, A., Gerbersdorf, S.U., Nowak, W., Chen, P.J., 2020. Floating
581 photovoltaic plants: Ecological impacts versus hydropower operation flexibility. Energy Conversion
582 and Management 206, 112414.

583
584 Holm, A., 2017. Floating Solar Photovoltaics Gaining Ground. https://www.nrel.gov/technical-
585 assistance/blog/posts/floating-solar-photovoltaics-gaining-ground.html. (Accessed 09/11/2017
586 2017).

587
588 Hondzo, M., Stefan, H.G., 1993. Lake Water Temperature Simulation-Model. Journal of Hydraulic
589 Engineering 119(11), 1251-1273.

590
591 Huisman, J., van Oostveen, P., Weissing, F.J., 1999. Critical depth and critical turbulence: Two
592 different mechanisms for the development of phytoplankton blooms. Limnol Oceanogr 44(7), 1781-
593 1787.

594
595 Huisman, J., Sharples, J., Stroom, J.M., Visser, P.M., Kardinaal, W.E.A., Verspagen, J.M.H., Sommeijer,
596 B., 2004. Changes in turbulent mixing shift competition for light between phytoplankton species.
597 Ecology 85(11), 2960-2970.

598
599 IEA, 2019. 2019 Snapshot of Global PV Markets, Strategic PV Analysis and Outreach.

600
601 Jäger, C.G., Diehl, S., Schmidt, G.M., 2008. Influence of water-column depth and mixing on
602 phytoplankton biomass, community composition, and nutrients. Limnol Oceanogr 53(6), 2361-2373.

603
604 Jesson, D.A., Le Page, B.H., Mulheron, M.J., Smith, P.A., Wallen, A., Cocks, R., Farrow, J., Whiter, J.T.,
605 2010. Thermally induced strains and stresses in cast iron water distribution pipes: an experimental
606 investigation. J Water Supply Res T 59(4), 221-229.

607
608 Jurvelius, J., Marjomki, T.J., 2008. Night, day, sunrise, sunset: do fish under snow and ice recognize
609 the difference? Freshwater Biology 53(11), ???-???

610
611 Kalff, J., 2002. Limnology : inland water ecosystems. Prentice Hall, Upper Saddle River, NJ.

612
613 Knoll, L.B., Sharma, S., Denfeld, B.A., Flaim, G., Hori, Y., Magnuson, J.I., Straile, D., Weyhenmeyer,
614 G.A., 2019. Consequences of lake and river ice loss on cultural ecosystem services. Limnol Oceanogr
615 Lett 4(5), 119-131.

616
617 Kraemer, B.M., Anneville, O., Chandra, S., Dix, M., Kuusisto, E., Livingstone, D.M., Rimmer, A.,
618 Schladow, S.G., Silow, E., Sitoki, L.M., Tamatamah, R., Vadeboncoeur, Y., McIntyre, P.B., 2015.
619 Morphometry and average temperature affect lake stratification responses to climate change.
620 Geophys. Res. Lett. 42(12), 4981-4988.

621

622 Kraemer, B.M., Chandra, S., Dell, A.I., Dix, M., Kuusisto, E., Livingstone, D.M., Schladow, S.G., Silow,
623 E., Sitoki, L.M., Tamatamah, R., McIntyre, P.B., 2017. Global patterns in lake ecosystem responses to
624 warming based on the temperature dependence of metabolism. Glob Chang Biol 23(5), 1881-1890.
625
626 Lee, N., Grunwald, U., Rosenlieb, E., Mirletz, H., Aznar, A., Spencer, R., Cox, S., 2020. Hybrid floating
627 solar photovoltaics-hydropower systems: Benefits and global assessment of technical potential.
628 Renew. Energy 162, 1415-1427.
629
630 Leppäranta, M., 1993. A review of analytical models of sea-ice growth. Atmosphere-Ocean 31(1),
631 123-138.
632
633 Lerman, A., Imboden, D.M., Gat, J.R., 1995. Physics and Chemistry of Lakes. Springer, Berlin.
634
635 Lewis, W.M., 1987. Tropical Limnology. Annual Review of Ecology and Systematics 18(1), 159-184.
636
637 Liu, L., Wang, Q., Lin, H., Li, H., Sun, Q., wennersten, R., 2017. Power Generation Efficiency and
638 Prospects of Floating Photovoltaic Systems. Energy Procedia 105, 1136-1142.
639
640 Livingstone, D.M., Adrian, R., 2009. Modeling the duration of intermittent ice cover on a lake for
641 climate-change studies. Limnol Oceanogr 54(5), 1709-1722.
642
643 Maberly, S.C., Elliott, J.A., 2012. Insights from long-term studies in the Windermere catchment:
644 external stressors, internal interactions and the structure and function of lake ecosystems.
645 Freshwater Biology 57(2), 233-243.
646
647 Macintyre, S., 1993. Vertical Mixing in a Shallow, Eutrophic Lake - Possible Consequences for the
648 Light Climate of Phytoplankton. Limnol Oceanogr 38(4), 798-817.
649
650 Maestre-Valero, J.F., Martinez-Alvarez, V., Nicolas, E., 2013. Physical, chemical and microbiological
651 effects of suspended shade cloth covers on stored water for irrigation. Agricultural Water
652 Management 118, 70-78.
653
654 Meis, S., Thackeray, S.J., Jones, I.D., 2009. Effects of recent climate change on phytoplankton
655 phenology in a temperate lake. Freshwater Biology 54(9), 1888-1898.
656
657 Maltby, E., Ormerod, S., Acreman, M., Dunbar, M., Jenkins, A., Maberly, S., Newman, J., Blackwell,
658 M., Ward, R., 2011. Freshwaters: openwaters, wetlands and floodplains, UK National Ecosystem
659 Assessment: understanding nature's value to society. UNEP-WCMC, Cambridge, UK, pp. 295-360.
660
661 Moriasi, D.N., Arnold, J.G., Van Liew, M.W., Bingner, R.L., Harmel, R.D., Veith, T.L., 2007. Model
662 evaluation guidelines for systematic quantification of accuracy in watershed simulations.
663 Transactions of the Asabe 50(3), 885-900.
664

Mathijssen, D., Hofs, B., Spierenburg-Sack, E., van Asperen, R., van der Wal, B., Vreeburg, J., Ketelaars, H., 2020. Potential impact of floating solar panels on water quality in reservoirs; pathogens and leaching. Water Pract Technol 15(3), 807-811.

Nash, J.E., Sutcliffe, J.V., 1970. River flow forecasting through conceptual models part I — A discussion of principles. J. Hydrol. 10(3), 282-290.

National River Flow Archive, 2018. 73010 - Leven at Newby Bridge. National River Flow Archive, National River Flow Archive.

North, R.P., North, R.L., Livingstone, D.M., Koster, O., Kipfer, R., 2014. Long-term changes in hypoxia and soluble reactive phosphorus in the hypolimnion of a large temperate lake: consequences of a climate regime shift. Glob Chang Biol 20(3), 811-823.

O'Neil, J.M., Davis, T.W., Burford, M.A., Gobler, C.J., 2012. The rise of harmful cyanobacteria blooms: The potential roles of eutrophication and climate change. Harmful Algae 14, 313-334.

O'Reilly, C.M., Sharma, S., Gray, D.K., Hampton, S.E., Read, J.S., Rowley, R.J., Schneider, P., Lenters, J.D., McIntyre, P.B., Kraemer, B.M., Weyhenmeyer, G.A., Straile, D., Dong, B., Adrian, R., Allan, M.G., Anneville, O., Arvola, L., Austin, J., Bailey, J.L., Baron, J.S., Brookes, J.D., de Eyto, E., Dokulil, M.T., Hamilton, D.P., Havens, K., Hetherington, A.L., Higgins, S.N., Hook, S., Izmest'eva, L.R., Joehnk, K.D., Kangur, K., Kasprzak, P., Kumagai, M., Kuusisto, E., Leshkevich, G., Livingstone, D.M., MacIntyre, S., May, L., Melack, J.M., Mueller-Navarra, D.C., Naumenko, M., Noges, P., Noges, T., North, R.P., Plisnier, P.D., Rigosi, A., Rimmer, A., Rogora, M., Rudstam, L.G., Rusak, J.A., Salmaso, N., Samal, N.R., Schindler, D.E., Schladow, S.G., Schmid, M., Schmidt, S.R., Silow, E., Soylu, M.E., Teubner, K., Verburg, P., Voutilainen, A., Watkinson, A., Williamson, C.E., Zhang, G.Q., 2015. Rapid and highly variable warming of lake surface waters around the globe. Geophys. Res. Lett. 42(24), 10773-10781.

Oke, T.R., 2002. Boundary layer climates. Routledge.

Oliveira-Pinto, S., Stokkermans, J., 2020. Assessment of the potential of different floating solar technologies - Overview and analysis of different case studies. Energy Conversion and Management 211, 112747.

Ozkundakci, D., Gsell, A.S., Hintze, T., Tauscher, H., Adrian, R., 2016. Winter severity determines functional trait composition of phytoplankton in seasonally ice-covered lakes. Glob Chang Biol 22(1), 284-298.

Paerl, H.W., Paul, V.J., 2012. Climate change: links to global expansion of harmful cyanobacteria. Water Res 46(5), 1349-1363.

Pinto, P.D., Allende, L., O'Farrell, I., 2007. Influence of free-floating plants on the structure of a natural phytoplankton assemblage: an experimental approach. Journal of Plankton Research 29(1), 47-56.

710 Ramsbottom, A., 1976. Depth charts ofthe Cumbrian lakes. Sci. Publ. Freshwater Biol. Assoc.

711
712 Read, J.S., Hamilton, D.P., Desai, A.R., Rose, K.C., MacIntyre, S., Lenters, J.D., Smyth, R.L., Hanson,
713 P.C., Cole, J.J., Staehr, P.A., Rusak, J.A., Pierson, D.C., Brookes, J.D., Laas, A., Wu, C.H., 2012. Lake-size
714 dependency of wind shear and convection as controls on gas exchange. Geophys. Res. Lett. 39, 5.

715
716 Read, J.S., Hamilton, D.P., Jones, I.D., Muraoka, K., Winslow, L.A., Kroiss, R., Wu, C.H., Gaiser, E.,
717 2011. Derivation of lake mixing and stratification indices from high-resolution lake buoy data.
718 Environmental Modelling & Software 26(11), 1325-1336.

719
720 Redón-Santafé, M., Ferrer-Gisbert, P.-S., Sánchez-Romero, F.-J., Torregrosa Soler, J.B., Gozalvez, F.,
721 Javier, J., Ferrer Gisbert, C.M., 2014. Implementation of a photovoltaic floating cover for irrigation
722 reservoirs. Journal of cleaner production 66, 568-570.

723
724 REN21, 2020. Renewables 2020 Global Status Report. Paris.

725
726 Reynaud, A., Lanzanova, D., 2017. A Global Meta-Analysis of the Value of Ecosystem Services
727 Provided by Lakes. Ecol Econ 137, 184-194.

728
729 Riley, M.J., Stefan, H.G., 1988. Minlake - a Dynamic Lake Water-Quality Simulation-Model. Ecological
730 Modelling 43(3-4), 155-182.

731
732 Rooney, G.G., Jones, I.D., 2010. Coupling the 1-D lake model FLake to the community land-surface
733 model JULES. Boreal Environment Research 15(5), 501-512.

734
735 Sacramento, E.M.d., Carvalho, P.C.M., de Araújo, J.C., Riffel, D.B., Corrêa, R.M.d.C., Pinheiro Neto,
736 J.S., 2015. Scenarios for use of floating photovoltaic plants in Brazilian reservoirs. IET Renewable
737 Power Generation 9(8), 1019-1024.

738
739 Sahu, A., Yadav, N., Sudhakar, K., 2016. Floating photovoltaic power plant: A review. Renew. Sust.
740 Energ. Rev. 66, 815-824.

741
742 Saloranta, T.M., 2000. Modeling the evolution of snow, snow ice and ice in the Baltic Sea. Tellus
743 Series a-Dynamic Meteorology and Oceanography 52(1), 93-108.

744
745 Saloranta, T., Andersen, T., 2004. MyLake v1.1: technical documentation & user's guide, Norwegian
746 Institute for Water Research. Norwegian Institute for Water Research.

747
748 Saloranta, T.M., Andersen, T., 2007. MyLake - A multi-year lake simulation model code suitable for
749 uncertainty and sensitivity analysis simulations. Ecological Modelling 207(1), 45-60.

750
751 Santafe, M.R., Gisbert, P.S.F., Romero, F.J.S., Soler, J.B.T., Gozalvez, J.J.F., Gisbert, C.M.F., 2014.
752 Implementation of a photovoltaic floating cover for irrigation reservoirs. Journal of Cleaner
753 Production 66, 568-570.

Solar Asset Management, 2018. TOP 70 FLOATING SOLAR PV PLANTS. https://solarassetmanagement.asia/news/top-70-floating-solar-pv-plants. (Accessed July 2018).

Solarplaza, 2019. A Comprehensive Overview of 200+ Global Floating Solar Plants. pp. 1 - 19.

Stiubiener, U., da Silva, T.C., Trigoso, F.B.M., Benedito, R.D., Teixeira, J.C., 2020. PV power generation on hydro dam's reservoirs in Brazil: A way to improve operational flexibility. Renew. Energy 150, 765-776.

Sulaeman, S., Brown, E., Quispe-Abad, R., Muller, N., 2021. Floating PV system as an alternative pathway to the amazon dam underproduction. Renew. Sust. Energ. Rev. 135, 110082.

Taboada, M.E., Caceres, L., Graber, T.A., Galleguillos, H.R., Cabeza, L.F., Rojas, R., 2017. Solar water heating system and photovoltaic floating cover to reduce evaporation: Experimental results and modeling. Renew. Energy 105, 601-615.

Talling, J.F., 2001. Environmental controls on the functioning of shallow tropical lakes. Hydrobiologia 458(1), 1-8.

Thackeray, S.J., Henrys, P.A., Feuchtmayr, H., Jones, I.D., Maberly, S.C., Winfield, I.J., 2013. Food web de-synchronization in England's largest lake: an assessment based on multiple phenological metrics. Glob Chang Biol 19(12), 3568-3580.

Thackeray, S.J., Jones, I.D., Maberly, S.C., 2008. Long-term change in the phenology of spring phytoplankton: species-specific responses to nutrient enrichment and climatic change. Journal of Ecology 96(3), 523-535.

Tina, G.M., Scavo, F.B., Merlo, L., Bizzarri, F., 2021. Comparative analysis of monofacial and bifacial photovoltaic modules for floating power plants. Applied Energy 281, 116084.

Tranvik, L.J., Downing, J.A., Cotner, J.B., Loiselle, S.A., Striegl, R.G., Ballatore, T.J., Dillon, P., Finlay, K., Fortino, K., Knoll, L.B., Kortelainen, P.L., Kutser, T., Larsen, S., Laurion, I., Leech, D.M., McCallister, S.L., McKnight, D.M., Melack, J.M., Overholt, E., Porter, J.A., Prairie, Y., Renwick, W.H., Roland, F., Sherman, B.S., Schindler, D.W., Sobek, S., Tremblay, A., Vanni, M.J., Verschoor, A.M., von Wachenfeldt, E., Weyhenmeyer, G.A., 2009. Lakes and reservoirs as regulators of carbon cycling and climate. Limnol Oceanogr 54(6), 2298-2314.

Visser, M.E., Both, C., 2005. Shifts in phenology due to global climate change: the need for a yardstick. Proc Biol Sci 272(1581), 2561-2569.

Walsby, A.E., Hayes, P.K., Boje, R., Stal, L.J., 1997. The selective advantage of buoyancy provided by gas vesicles for planktonic cyanobacteria in the Baltic Sea. New Phytologist 136(3), 407-417.

798 Wetzel, R.G., 2001. Limnology: lake and river ecosystems, 3rd ed. Academic Press, San Diego.

799
800 Woolway, R.I., Jones, I.D., Feuchtmayr, H., Maberly, S.C., 2015a. A comparison of the diel variability
801 in epilimnetic temperature for five lakes in the English Lake District. Inland Waters 5(2), 139-154.

802
803 Woolway, R.I., Jones, I.D., Hamilton, D.P., Maberly, S.C., Muraoka, K., Read, J.S., Smyth, R.L.,
804 Winslow, L.A., 2015b. Automated calculation of surface energy fluxes with high-frequency lake buoy
805 data. Environmental Modelling & Software 70, 191-198.

806
807 Woolway, R.I., Jones, I.D., Maberly, S.C., French, J.R., Livingstone, D.M., Monteith, D.T., Simpson,
808 G.L., Thackeray, S.J., Andersen, M.R., Battarbee, R.W., DeGasperi, C.L., Evans, C.D., de Eyto, E.,
809 Feuchtmayr, H., Hamilton, D.P., Kernan, M., Krokowski, J., Rimmer, A., Rose, K.C., Rusak, J.A., Ryves,
810 D.B., Scott, D.R., Shilland, E.M., Smyth, R.L., Staehr, P.A., Thomas, R., Waldron, S., Weyhenmeyer,
811 G.A., 2016. Diel Surface Temperature Range Scales with Lake Size. PLoS One 11(3), e0152466.

812
813 Woolway, R.I., Meinson, P., Nõges, P., Jones, I.D., Laas, A., 2017. Atmospheric stilling leads to
814 prolonged thermal stratification in a large shallow polymictic lake. Climatic Change 141(4), 759-773.

815
816 Woolway, R.I., Merchant, C.J., 2019. Worldwide alteration of lake mixing regimes in response to
817 climate change. Nat. Geosci. 12(4), 271-+.

818
819 Woolway, R.I., Verburg, P., Lenters, J.D., Merchant, C.J., Hamilton, D.P., Brookes, J., de Eyto, E., Kelly,
820 S., Healey, N.C., Hook, S., Laas, A., Pierson, D., Rusak, J.A., Kuha, J., Karjalainen, J., Kallio, K., Lepisto,
821 A., Jones, I.D., 2018. Geographic and temporal variations in turbulent heat loss from lakes: A global
822 analysis across 45 lakes. Limnol Oceanogr 63(6), 2436-2449.

823
824 Woolway, R.I., Verburg, P., Merchant, C.J., Lenters, J.D., Hamilton, D.P., Brookes, J., Kelly, S., Hook,
825 S., Laas, A., Pierson, D., Rimmer, A., Rusak, J.A., Jones, I.D., 2017. Latitude and lake size are
826 important predictors of over-lake atmospheric stability. Geophys. Res. Lett. 44(17), 8875-8883.

827
828 Woolway, R.I., Weyhenmeyer, G.A., Schmid, M., Dokulil, M.T., de Eyto, E., Maberly, S.C., May, L.,
829 Merchant, C.J., 2019. Substantial increase in minimum lake surface temperatures under climate
830 change. Climatic Change 155(1), 81-94.

831
832 World Bank Group, ESMAP, SERIS, 2018. Where Sun Meets Water : Floating Solar Market Report.
833 Washington, D.C.

834
835 World Bank Group, ESMAP, SERIS, 2019. Where Sun Meets Water: Floating Solar Handbook for
836 Practitioners. Washington, DC.

837
838 Yadav, N., Gupta, M., Sudhakar, K., Ieee, 2016. Energy Assessment of Floating Photovoltaic System.

839
840 Yankova, Y., Neuenschwander, S., Koster, O., Posch, T., 2017. Abrupt stop of deep water turnover
841 with lake warming: Drastic consequences for algal primary producers. Sci Rep 7(1), 13770.

Zhang, N., Jiang, T., Guo, C., Qiao, L.F., Ji, Q., Yin, L.Q., Yu, L.M., Murto, P., Xu, X.F., 2020. High-performance semitransparent polymer solar cells floating on water: Rational analysis of power generation, water evaporation and algal growth. Nano Energy 77, 105111.

Zhou, Y.L., Chang, F.J., Chang, L.C., Lee, W.D., Huang, A., Xu, C.Y., Guo, S.L., 2020. An advanced complementary scheme of floating photovoltaic and hydropower generation flourishing water-food-energy nexus synergies. Applied Energy 275, 115389.

Ziar, H., Prudon, B., Lin, F.Y., Roeffen, B., Heijkoop, D., Stark, T., Teurlincx, S., Domis, L.D., Goma, E.G., Extebarria, J.G., Alavez, I.N., van Tilborg, D., van Laar, H., Santbergen, R., Isabella, O., 2020. Innovative floating bifacial photovoltaic solutions for inland water areas. Prog Photovoltaics.